



# Journal of Composites and Compounds

## Simple synthesis of $\text{Fe}_3\text{O}_4@\text{Fe}_3\text{S}_4$ nanocomposites coated with polyindole-polythiophene for high-performance supercapacitor

AliAkbar Asgharinezhad <sup>a\*</sup> , Ehsan Niknam <sup>a</sup>, Afsanehsadat Larimi <sup>a</sup>

<sup>a</sup> Chemistry and Process Engineering Department, Niroo Research Institute (NRI), Tehran, Iran

### ABSTRACT

To prevent a major energy crisis in the near future, it is necessary to assemble efficient electrochemical energy storage devices such as supercapacitors. Herein, a  $\text{Fe}_3\text{O}_4@\text{Fe}_3\text{S}_4$  nanocomposites coated with polyindole-polythiophene on nickel foam (NF) has been prepared by following a low facile, multistep method. In terms of structural and electrochemical performance, the nanocomposites have been investigated. The electrochemical properties of as fabricated  $\text{Fe}_3\text{O}_4@\text{Fe}_3\text{S}_4@\text{PIn-PTH}$  are studied in 2M KOH. A specific capacitance of  $100.83 \text{ F g}^{-1}$  at a current density of  $2 \text{ A g}^{-1}$ . The results of the synthesized sample in comparison with  $\text{Fe}_3\text{O}_4$  show that using sulfide metal and polymer component improve the electrochemical performance. These characteristics of  $\text{Fe}_3\text{O}_4@\text{Fe}_3\text{S}_4@\text{PIn-PTH}$  as the active material illustrate a suitable performance as a cathode material for electrochemical energy storage.

©2023 UGPH.

Peer review under responsibility of UGPH.

### ARTICLE INFORMATION

#### Article history:

Received 11 January 2023

Received in revised form 01 March 2023

Accepted 26 March 2023

#### Keywords:

Supercapacitor

Nanocomposite

$\text{Fe}_3\text{O}_4$

$\text{Fe}_3\text{S}_4$

Active Material Synthesis

### 1. Introduction

Indiscriminate consumption of fossil energy due to the increase in consumption and development of industries has caused many problems, including the reduction of fossil fuel reserves as well as problems such as environmental pollution. Therefore, there is a need to develop clean and renewable energy generators such as solar cells, wind turbines, etc., and considering the dependence of these energies on atmospheric conditions, the issue of storing these energies as a priority is given. According to their characteristics, electrochemical energy storage devices are classified into various categories, such as supercapacitors, batteries, capacitors, and fuel cells [1–6].

Supercapacitors, which have a high power density, a long functional life, and no need for special maintenance equipment, have been the focus of industrial and academic research in recent years. The mechanism of operation of supercapacitors is based on the exchange of electrons between the electrolyte and the electrode of the supercapacitor, and this process depends on the active materials used in the electrode. Common electrode materials in the preparation of transition metal oxides and sulfides are conductive polymers or carbon materials with a large surface area [7–12] as they present multifold advantages of high power density, fast charging–discharging, and long cyclic stability. However, the intrinsically low energy density inherent to traditional supercapacitors severely limits their widespread applications, triggering researchers to explore new types of supercapacitors with improved performance. Asymmetric supercapacitors (ASCs).

Due to their ability to provide high capacity (compared to the oxide

state, due to the lower electronegativity of sulfur compared to oxygen), metal sulfides are among the materials that are of interest in research in supercapacitor studies as active electrode materials. In these materials, based on fast and reversible reactions on the surface of the active material, it produces this capacity. In order to achieve high energy density and power, materials must have reversible reactions with electrolytes at high speeds. However, research is aimed at improving the properties of active materials used in supercapacitor electrodes. One of the things that is of interest in research today in order to improve the properties of these materials is the use of nanomaterials. Due to their porous and regular structure, these materials cause the structure to become porous and subsequently increase the electron exchange between the electrode and the electrolyte, which leads to an improvement in the electrochemical performance of the supercapacitor [13–15].

Another desirable thing in the synthesis of active materials is to functionalize the surface and increase the hydrophilic property due to the improvement of electron exchange in the electrochemical process, which is possible by coating the synthesized structure with a polymer layer. For the synthesis of iron oxide magnetic particles in controlled atmospheres, various methods such as hydrothermal, co-precipitation, sol-gel, and solvothermal are used. Among the mentioned methods, the co-precipitation method is a suitable option for synthesis on a large and industrial scale due to its ease of implementation and lower cost [16–18] a novel core-shell structure is developed based on CoS deposited on NiS nanosheets, which involves hydrothermal and electrodeposition method. The micromorphology of the composite electrode can be optimized by adjusting the cycles of electrodeposition. Taking advantages of the high-

\* Corresponding author: AliAkbar Asgharinezhad; E-mail: [aasgharinezhad@nri.ac.ir](mailto:aasgharinezhad@nri.ac.ir)

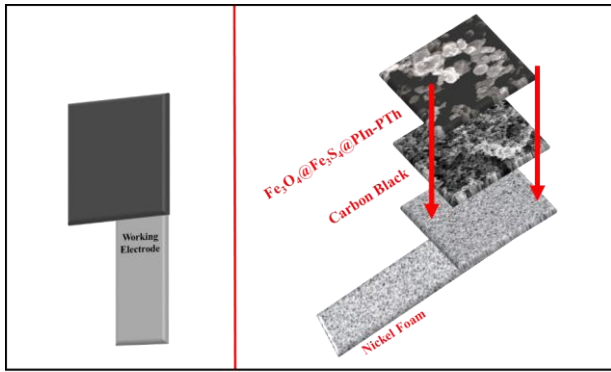


Fig. 1. Fabricated working electrode with its components.

ly conductive, open framework of the core-shell nanolayer, the 5-NiS@CoS electrode shows a specific capacitance of  $1210 \text{ F g}^{-1}$  at a current density of  $1 \text{ A g}^{-1}$  (retaining 82% from 1 to  $10 \text{ A g}^{-1}$ , while NiS substrate is only 39%).

Using two 2 and 3 valent iron salts and the co-precipitation method, particles for use as the active material in the hybrid supercapacitor electrode are prepared in this study. There is a need for identification and functional tests for electrochemical performance and electron exchange between electrode and electrolyte.

In this work,  $\text{Fe}_3\text{O}_4@\text{Fe}_3\text{S}_4$  nanocomposites coated with polyindole-polythiophene ( $\text{Fe}_3\text{O}_4@\text{Fe}_3\text{S}_4@\text{PIn-PTH}$ ) are synthesized as active materials and evaluated for supercapacitor application. This study consists of material Characterization and electrochemical investigation.

## 2. Experimental

### 2.1. Material and Electrode

Magnetic  $\text{Fe}_3\text{S}_4$  nanoparticles (magnetite) were synthesized by the coprecipitation method. First, 2.7 g of  $\text{FeCl}_3$  salt and 7.84 g of  $\text{FeCl}_2 \cdot 6\text{H}_2\text{O}$  with a Fe (III) to Fe (II) molar ratio of 2:1. Ions were dissolved in 400 ml of deionized water, and the solution was deoxygenated for 10 minutes before being heated to 80 degrees Celsius during simultaneous deoxygenation. After that, 20 ml of 25% ammonium hydroxide solution was added to the stirring solution (1000 rpm). The presence of oxygen causes the formation of  $\text{Fe}_2\text{O}_3$  nanoparticles, which are not very desirable because they have a lower specific surface area and lower magnetic properties than  $\text{Fe}_3\text{O}_4$ . After the end of the reaction, the precipitate of magnetite nanoparticles was separated from the reaction environment with a magnet and washed several times with deionized water, and finally the obtained nanoparticles were dried at ambient temperature.

To prepare magnetic nanoparticles covered with a polymer layer and to increase the hydrophilic property and functionalize its surface, a mixture of thiophene and indole was added to the magnetic nanoparticles prepared in the previous step by the chemical oxidation polymerization method in an aqueous medium using Fe (III) chloride synthesized as an oxidant. Thus, 0.75 grams of magnetic nanoparticles were added to 100 ml of deionized water and subjected to ultrasonic waves for 10 minutes. Next, a solution consisting of 0.3 ml of thiophene and 0.19 g of indole was added to the reaction mixture, and the resulting mixture was stirred for 10 minutes. Next, 1.3516 grams of  $\text{FeCl}_3$ , which was dissolved in 25 ml of deionized water, was added dropwise to the aforementioned mixture over a period of 30 minutes, and the polymerization process was carried out for 6 hours at a temperature of 30 degrees Celsius. Grad continued. Then, in order to stop the polymerization reaction, acetone was added to the reaction mixture. Finally, the functionalized adsorbent was collected with a magnet and washed several times with deionized water and methanol to remove impurities.

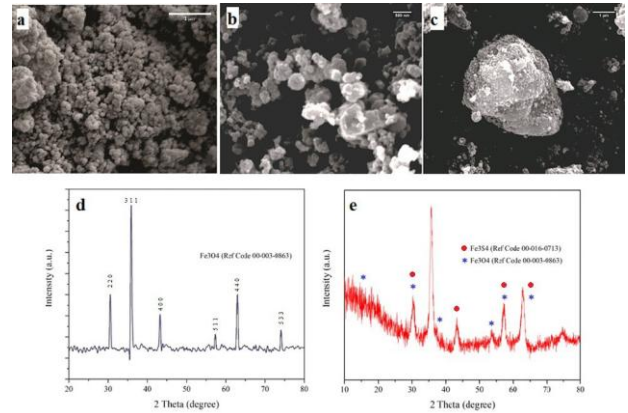


Fig. 2. SEM images of (a)  $\text{Fe}_3\text{O}_4$  and (b-c)  $\text{Fe}_3\text{O}_4@\text{Fe}_3\text{S}_4@\text{PIn-PTH}$ , XRD patterns of (d)  $\text{Fe}_3\text{O}_4$  and (e)  $\text{Fe}_3\text{O}_4@\text{Fe}_3\text{S}_4@\text{PIn-PTH}$ .

In order to produce the sulfide component, 0.25 g of  $\text{Fe}_3\text{O}_4@\text{PIn-PTH}$  in 300 ml of ethylene glycol was subjected to ultrasonic waves for 15 minutes to obtain a homogeneous mixture. Next, 2.25 g of thiourea was dissolved in 40 ml of ethylene glycol and added to the reaction mixture. The intended reaction continued for 4 hours at 150°C, and finally the synthesized material was washed with enough water and ethanol to remove impurities and unreacted materials.

### 2.2. Material Characterization and electrochemical investigation

The morphological investigation of the samples was done by scanning electron microscopy (SEM) (FEI SEM QUANTA 200). For electrochemical performance, Palmsens (Palmsens 4) was used for all evaluations, such as cyclic voltammetry (CV), charge and discharge (CD), and electrochemical impedance spectroscopy (EIS) in 2 M KOH as the electrolyte. The electrodes (active materials coated on nickel foam) are applied as a working electrode linking a reference electrode of Ag/AgCl. Platinum (Pt) wire was employed as a counter electrode in three-electrode cell mode. The active materials coated on nickel foam as working electrode was made as follows: active material, acetylene black, and polyvinylidene fluoride with mass ratio of 80:15:5 in N-Methyl-2-pyrrolidone on washed nickel foam electrode with thickness of 0.2 cm, for fabrication of samples as working electrode. Then, the slurries were coated on Ni foam with brushing method. The mass of slurry on the electrode was  $3 \text{ mg cm}^{-2}$  on  $1 \text{ cm}^2$ . Finally, the fabricated electrodes dried at 100 °C for 150 min. Fabricated electrode can be seen in Fig.1. The following equations are used to determine the specific capacitance ( $C_{sp}$ ) [19]  $\text{Fe}_3\text{O}_4@\text{C}$  nanoparticles were synthesized by thermal decomposition. Then these synthesized nanoparticles, 20–30 nm in size were processed in a solution of glucose at 200 °C during 12 h, which led to an unexpected phenomenon; the nanoparticles self-assembled into large conglomerates of a regular shape of about 300 nm in size. The morphology and features of the magnetic properties of the obtained hybrid nanoparticles were characterized by transmission electron microscopy, differential thermo-gravimetric analysis, vibrating sample magnetometer, magnetic circular dichroism and Mössbauer spectroscopy. It was shown that the magnetic core of  $\text{Fe}_3\text{O}_4@\text{C}$  nanoparticles was nano-crystalline, corresponding to the  $\text{Fe}_3\text{O}_4$  phase. The  $\text{Fe}_3\text{O}_4@\text{C}$  nanoparticles presumably contain  $\text{Fe}_3\text{O}_4$  phase (80%,

$$C_{sp} = \frac{I \times \Delta t}{m \times \Delta V} \quad (1)$$

## 3. Results and discussion

### 3.1. Structural Characterization

As can be seen in Fig.2 (a-c), based on the scanning electron micro-

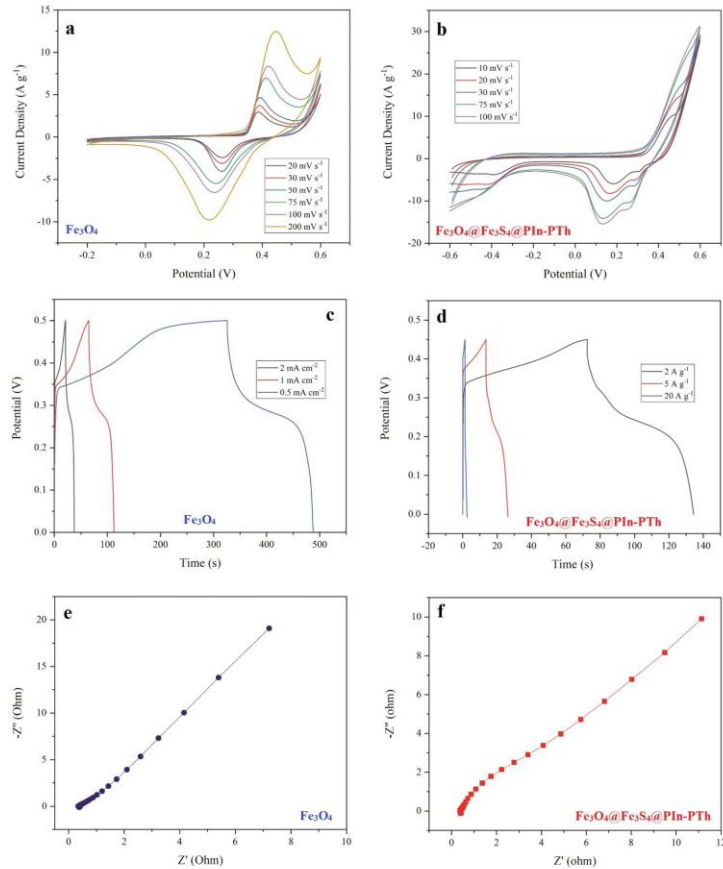


**Fig. 3.** (a-b) CV curves, (c-d) GCD curves, (e-f) EIS curves of  $\text{Fe}_3\text{O}_4$  and  $\text{Fe}_3\text{O}_4@\text{Fe}_3\text{S}_4@\text{PIn-PTh}$ .

scope images of the synthesized nanoparticles, a spherical morphology with relatively homogeneous particle distribution is seen. One of the things that prevents a completely desirable morphology in these situations is the lack of complete interaction between the reacting materials. The dimensions of the synthesized particles are in nanometers, which causes a favorable interaction with the electrolyte in order to exchange electrons. According to previous researches, nanometer dimensions and spherical morphology for active materials, due to having a more specific area, will improve the electrochemical performance of these materials in supercapacitor applications [20–22]. In comparison with  $\text{Fe}_3\text{O}_4$  sample, particles have more diameter because of having sulfide particle on their surface and a cover of PIn-PTh. X-ray diffraction test has been used for phase identification (Fig.2 (d-e)). By analyzing the diffraction pattern resulting from this test by X'Pert HighScore software, iron oxide ( $\text{Fe}_3\text{O}_4$ ) in  $\text{Fe}_3\text{O}_4$  sample and a complex of  $\text{Fe}_3\text{O}_4$  and  $\text{Fe}_3\text{S}_4$  phases have been identified in  $\text{Fe}_3\text{O}_4@\text{Fe}_3\text{S}_4@\text{PIn-PTh}$  sample [15], [23–26]. As can be seen, the intensity of  $\text{Fe}_3\text{O}_4$  peaks were decreased by using sulfide element and the pattern looks more like amorphous phase which this causes more active sites for electron transition. Another benefit of turning oxide component as anion with sulfide is having lower electronegativity which enhances electrochemical performance [13].

Firstly,  $\text{Fe}_3\text{O}_4$  and  $\text{Fe}_3\text{O}_4@\text{Fe}_3\text{S}_4@\text{PIn-PTh}$  were examined by the cyclic voltammetry (CV) curves. Fig.3 (a-b) illustrate that  $\text{Fe}_3\text{O}_4@\text{Fe}_3\text{S}_4@\text{PIn-PTh}$  possesses a higher CV area compared to another sample, which leads to high capacitance performance. Furthermore, the CV curve of  $\text{Fe}_3\text{O}_4@\text{Fe}_3\text{S}_4@\text{PIn-PTh}$  has one more peak which is belonged to PIn-PTh component and electrolyte reaction [27, 28]. Moreover, the potential range of  $\text{FeO}^{3-}_4@\text{Fe}_3\text{S}_4^{3-}$  @ PIn-PTh is more than  $\text{Fe}_3\text{O}_4^{3-}$  which leads to work that wider range of potential. The scan rate of both sample

ranged from 5 to 200  $\text{mV s}^{-1}$ , and the corresponding current intensity of the peaks increased and shows the good electrochemical reversibility. Both samples were evaluated by the galvanostatic charge-discharge (GCD) technique in 2 M KOH solution at different range of current density (Fig.3 (c-d)). Both samples' curves show a nonlinear charge-discharge profile that confirmed that the pseudocapacitance type of mechanism. The performance of  $\text{Fe}_3\text{O}_4@\text{Fe}_3\text{S}_4@\text{PIn-PTh}$  is better than  $\text{Fe}_3\text{O}_4$  and there is little iR drop (easy electron transformation) and can work at higher current densities with more capacity [29–33] which is constructed with many intercrossed nanorods, is successfully synthesized via a facile hydrothermal method. The achieved  $\text{Fe}_3\text{S}_4$  microspheres are evaluated as advanced anode materials for alkaline iron-based secondary batteries for the first time. Influences of hydrothermal temperature on the physical and electrochemical performances of  $\text{Fe}_3\text{S}_4$  particles are investigated systematically. It is found that the  $\text{Fe}_3\text{S}_4$  fabricated at 150 °C exhibits better electrochemical properties than the ones obtained at other temperatures, including higher discharge capacity, attractive high-rate capability and good cycling stability. At 0.2, 0.4, 1.0, 2.0, and 5.0 °C, the  $\text{Fe}_3\text{S}_4$  (150 °C). The specific capacitance of the  $\text{Fe}_3\text{O}_4@\text{Fe}_3\text{S}_4@\text{PIn-PTh}$  electrode ( $100.83 \text{ F g}^{-1}$  at  $2 \text{ A g}^{-1}$ ) is larger than the  $\text{Fe}_3\text{O}_4$  electrode ( $41.75 \text{ F g}^{-1}$ ).

Electrochemical impedance spectroscopy (EIS) was performed in a frequency range of 100 kHz–0.01 Hz with an AC voltage amplitude of 2 mV. In the EIS plots in Fig.3, for  $\text{Fe}_3\text{O}_4@\text{Fe}_3\text{S}_4@\text{PIn-PTh}$  sample, at high frequencies, a resistance of less than 1 ohm was observed for the sample, which indicates low internal resistance and good performance for electron exchange. At low frequencies, due to the approaching linear behavior and closeness to the vertical state, performance close to that of ideal supercapacitors can be seen. The results of EIS investigation for  $\text{Fe}_3\text{O}_4$  is worse compared to  $\text{Fe}_3\text{O}_4@\text{Fe}_3\text{S}_4@\text{PIn-PTh}$  (Fig.3 (e-f)) [34–37].

## 4. Conclusions

In summary, the  $\text{Fe}_3\text{O}_4@\text{Fe}_3\text{S}_4$  nanocomposites coated with poly-indole-polythiophene have been synthesized by a simple chemical method. According to structural characterization and electrochemical investigation, the results present that using sulfide and polymer component improves electrochemical performance. It is believed that  $\text{Fe}_3\text{O}_4@\text{Fe}_3\text{S}_4@\text{PIn-PTh}$  can be used as active material in electrochemical storage applications.

## Acknowledgments

The authors received no financial support for the research, authorship and/or publication of this article.

## Conflict of Interest

All authors declare no conflicts of interest in this paper.

## REFERENCES

- [1] A. Muzaffar, M.B. Ahamed, K. Deshmukh, J. Thirumalai, A review on recent advances in hybrid supercapacitors: Design, fabrication and applications, *Renewable and Sustainable Energy Reviews* 101 (2019) 123-145.
- [2] E. Niknam, H. Naffakh-Moosavy, S.E. Moosavifard, M.G. Afshar, Multi-shelled bimetal V-doped  $\text{Co}_3\text{O}_4$  hollow spheres derived from metal organic framework for high performance supercapacitors, *Journal of Energy Storage* 44 (2021) 103508.
- [3] U. Gulzar, S. Goriparti, E. Miele, T. Li, G. Maidecchi, A. Toma, F. De Angelis, C. Capiglia, R.P. Zaccaria, Next-generation textiles: from embedded supercapacitors to lithium ion batteries, *Journal of Materials Chemistry A* 4(43) (2016) 16771-16800.
- [4] E. Niknam, H. Naffakh-Moosavy, M.G. Afshar, Electrochemical performance of Nickel foam electrode in Potassium Hydroxide and Sodium Sulfate electrolytes for supercapacitor applications, *Journal of Composites and Compounds* 4(12) (2022) 149-152.
- [5] M.K. Aslam, T.S. AlGarni, M.S. Javed, S.S.A. Shah, S. Hussain, M. Xu, 2D MXene Materials for Sodium Ion Batteries: A review on Energy Storage, *Journal of Energy Storage* 37 (2021) 102478.
- [6] F. Ozel, H.S. Kilic, H. Coskun, I. Deveci, A. Sarilmaz, A. Balikcioglu, Y. Gundogdu, A. Aljabour, A. Ozen, S.Y. Gezgin, A. Houimi, A. Yar, M. Kus, M. Ersoz, A general review on the thiospinels and their energy applications, *Materials Today Energy* 21 (2021) 100822.
- [7] N. Choudhary, C. Li, J. Moore, N. Nagaiah, L. Zhai, Y. Jung, J. Thomas, Asymmetric Supercapacitor Electrodes and Devices, *Advanced Materials* 29(21) (2017) 1605336.
- [8] Z.S. Iro, C. Subramani, S.J.I.J.E.S. Dash, A brief review on electrode materials for supercapacitor, 11(12) (2016) 10628-10643.
- [9] S.Z. Golkhatmi, A. Sedghi, H.N. Miankushki, M. Khalaj, Structural properties and supercapacitive performance evaluation of the nickel oxide/graphene/polypyrrole hybrid ternary nanocomposite in aqueous and organic electrolytes, *Energy* 214 (2021) 118950.
- [10] H. Jiang, Y. Li, Y. Deng, W. Zhang, P. Dong, J. Zhang, In-situ-foaming synthesis of cheese-like  $\text{Fe}_3\text{O}_4@\text{TiC Tx}$  electrode material with both high energy and power density for Al/Zn-ion supercapacitors, *Journal of Materials Research and Technology* 23 (2023) 3547-3556.
- [11] L. Qu, L. Yang, Y. Ren, X. Ren, D. Fan, K. Xu, H. Wang, Y. Li, H. Ju, Q. Wei, A signal-off electrochemical sensing platform based on  $\text{Fe}_3\text{S}_4$ -Pd and pineal mesoporous bioactive glass for procalcitonin detection, *Sensors and Actuators B: Chemical* 320 (2020) 128324.
- [12] H. Mudila, P. Prasher, M. Kumar, A. Kumar, M.G.H. Zaidi, A. Kumar, Critical analysis of polyindole and its composites in supercapacitor application, *Materials for Renewable and Sustainable Energy* 8(2) (2019) 9-19.
- [13] E. Niknam, H. Naffakh-Moosavy, S.E. Moosavifard, M. Ghahraman Afshar, Amorphous V-doped  $\text{Co}_3\text{S}_4$  yolk-shell hollow spheres derived from metal-organic framework for high-performance asymmetric supercapacitors, *Journal of Alloys and Compounds* 895 (2022) 162720.
- [14] M. Karuppasamy, D. Muthu, Y. Haldorai, R.T. Rajendra Kumar, Solvothermal synthesis of  $\text{Fe}_3\text{S}_4@\text{graphene}$  composite electrode materials for energy storage, *Carbon Letters* 30(6) (2020) 667-673.
- [15] W. Meng, W. Chen, L. Zhao, Y. Huang, M. Zhu, Y. Huang, Y. Fu, F. Geng, J. Yu, X. Chen, C. Zhi, Porous  $\text{Fe}_3\text{O}_4$ /carbon composite electrode material prepared from metal-organic framework template and effect of temperature on its capacitance, *Nano Energy* 8 (2014) 133-140.
- [16] Y. Miao, X. Zhang, J. Zhan, Y. Sui, J. Qi, F. Wei, Q. Meng, Y. He, Y. Ren, Z. Zhan, Z. Sun, Hierarchical  $\text{NiS}@CoS$  with Controllable Core-Shell Structure by Two-Step Strategy for Supercapacitor Electrodes, *Advanced Materials Interfaces* 7(3) (2020) 1901618.
- [17] Y. Zhu, X. Yun, S. Wu, Z. Li, Y. Zhou, W. Zhong, C. Li, J. Li, M. Zhou, Mesoporous  $\text{Fe}_3\text{S}_4$  microparticles as a novel anode material for rechargeable alkaline aqueous batteries, *Ionics* 26(1) (2020) 105-113.
- [18] H. Talebi, A. Olad, R. Nosrati,  $\text{Fe}_3\text{O}_4/\text{PANI}$  nanocomposite core-shell structure in epoxy resin matrix for the application as electromagnetic waves absorber, *Progress in Organic Coatings* 163 (2022) 106665.
- [19] C.-R. Lin, O.S. Ivanova, I.S. Edelman, Y.V. Knyazev, S.M. Zharkov, D.A. Petrov, A.E. Sokolov, E.S. Svetlitsky, D.A. Velikanov, L.A. Solovyov, Y.-Z. Chen, Y.-T. Tseng, Carbon Double Coated  $\text{Fe}_3\text{O}_4@\text{C@C}$  Nanoparticles: Morphology Features, Magnetic Properties, Dye Adsorption, *Nanomaterials* 12(3) (2022) 376.
- [20] X. Du, C. Wang, M. Chen, Y. Jiao, J. Wang, Electrochemical Performances of Nanoparticle  $\text{Fe}_3\text{O}_4$ /Activated Carbon Supercapacitor Using KOH Electrolyte Solution, *Journal of Physical Chemistry C* 113(6) (2009) 2643-2646.
- [21] M. Aghazadeh, I. Karimzadeh, M.R. Ganjali, Electrochemical evaluation of the performance of cathodically grown ultra-fine magnetite nanoparticles as electrode material for supercapacitor applications, *Journal of Materials Science: Materials in Electronics* 28(18) (2017) 13532-13539.
- [22] M. Mazloum-Ardakani, F. Sabaghian, M. Yavari, A. Ebady, N. Sahraie, Enhance the performance of iron oxide nanoparticles in supercapacitor applications through internal contact of  $\alpha\text{-Fe}_2\text{O}_3@\text{CeO}_2$  core-shell, *Journal of Alloys and Compounds* 819 (2020) 152949.
- [23] Q. Liu, Z. Chen, R. Qin, C. Xu, J. Hou, Hierarchical mulberry-like  $\text{Fe}_3\text{S}_4/\text{Co}_9\text{S}_8$  nanoparticles as highly reversible anode for lithium-ion batteries, *Electrochimica Acta* 304 (2019) 405-414.
- [24] J. Sun, P. Zan, X. Yang, L. Ye, L. Zhao, Room-temperature synthesis of  $\text{Fe}_3\text{O}_4/\text{Fe}$ -carbon nanocomposites with Fe-carbon double conductive network as supercapacitor, *Electrochimica Acta* 215 (2016) 483-491.
- [25] B. Hu, Y. Wang, X. Shang, K. Xu, J. Yang, M. Huang, J. Liu, Structure-tunable  $\text{Mn}_3\text{O}_4\text{-Fe}_3\text{O}_4@\text{C}$  hybrids for high-performance supercapacitor, *Journal of Colloid and Interface Science* 581 (2021) 66-75.
- [26] A. Shokry, M. Karim, M. Khalil, S. Ebrahim, J. El Nady, Supercapacitor based on polymeric binary composite of polythiophene and single-walled carbon nanotubes, *Scientific Reports* 12(11278) (2022) 1-13.
- [27] S. Mozaffari, J. Behdani, S.M.B. Ghorashi, Synthesis of polyindole nanoparticles and its copolymers via emulsion polymerization for the application as counter electrode for dye-sensitized solar cells, *Polymer Bulletin* 79(8) (2022) 6777-6796.
- [28] A. Shokry, M. Karim, M. Khalil, S. Ebrahim, J. El Nady, Supercapacitor based on polymeric binary composite of polythiophene and single-walled carbon nanotubes, *J. Sci. Rep.* 12(11278) (2022) 1-13.
- [29] J. Li, J. Zheng, C. Wu, H. Zhang, T. Jin, F. Wang, Q. Li, E. Shangguan, Facile synthesis of  $\text{Fe}_3\text{S}_4$  microspheres as advanced anode materials for alkaline iron-based rechargeable batteries, *Journal of Alloys and Compounds* 874 (2021) 159873.
- [30] X. Wang, D. Jiang, C. Jing, X. Liu, K. Li, M. Yu, S. Qi, Y. Zhang, Biotemplate Synthesis of  $\text{Fe}_3\text{O}_4/\text{Polyaniline}$  for Supercapacitor, *Journal of Energy Storage* 30 (2020) 101554.
- [31] C. Wu, J. Zheng, J. Li, T. Jin, F. Wang, Q. Li, M. Chen, J. Qi, S. Gao, E. Shangguan,  $\text{Fe}_3\text{S}_4@\text{reduced graphene oxide}$  composites as novel anode materials for high performance alkaline secondary batteries, *Journal of Alloys and Compounds* 895 (2022) 162593.
- [32] W. Bao, C. Chen, W. Chen, X. Ding, Z. Si, Controllable synthesis of Ni-dotted  $\text{Fe}_3\text{S}_4$  with its superior wideband electromagnetic absorbing performance, *Journal of Materials Science: Materials in Electronics* 31(15) (2020) 12775-12782.
- [33] R.B. Choudhary, S. Ansari, B. Purty, Robust electrochemical performance of polypyrrole (PPy) and polyindole (PIn) based hybrid electrode materials for supercapacitor application: A review, *Journal of Energy Storage* 29 (2020) 101302.
- [34] M. Moradi, F. Hasanvandian, M. Ghahraman Afshar, A. Larimi, F. Khorasheh, E. Niknam, S. Rahman Setayesh, Incorporation of Fe in mixed  $\text{CoCu}$ -alkoxide hollow sphere for enhancing the electrochemical water oxidation performance, *Materials Today Chemistry* 22 (2021) 100586.
- [35] Y. Wang, Y. Lei, J. Li, L. Gu, H. Yuan, D. Xiao, Synthesis of 3D-Nanonet Hollow Structured  $\text{Co}_3\text{O}_4$  for High Capacity Supercapacitor, *ACS Applied Materials & Interfaces* 6(9) (2014) 6739-6747.
- [36] Y.-W. Li, W.-J. Zhang, J. Li, H.-Y. Ma, H.-M. Du, D.-C. Li, S.-N. Wang,

J.-S. Zhao, J.-M. Dou, L. Xu, Fe-MOF-Derived Efficient ORR/OER Bifunctional Electrocatalyst for Rechargeable Zinc–Air Batteries, *ACS Applied Materials & Interfaces* 12(40) (2020) 44710-44719.

[37] L. Wang, J. Yu, X. Dong, X. Li, Y. Xie, S. Chen, P. Li, H. Hou, Y. Song,

Three-Dimensional Macroporous Carbon/Fe<sub>3</sub>O<sub>4</sub>-Doped Porous Carbon Nanorods for High-Performance Supercapacitor, *ACS Sustainable Chemistry & Engineering* 4(3) (2016) 1531-1537.